

Review

Clinical Applications of In Vivo and Ex Vivo Confocal Microscopy

Stefania Guida ^{1,*}, Federica Arginelli ¹, Francesca Farnetani ¹, Silvana Ciardo ¹, Laura Bertoni ² ,
Marco Manfredini ¹, Nicola Zerbinati ³, Caterina Longo ^{1,4} and Giovanni Pellacani ^{1,5}

- ¹ Dermatology Unit, Department of Surgical, Medical, Dental and Morphological Sciences Related to Transplant, Oncology and Regenerative Medicine, University of Modena and Reggio Emilia, Via del Pozzo 71, 41125 Modena, Italy; federica.arginelli@unimore.it (F.A.); francesca.farnetani@unimore.it (F.F.); silvana.ciardo@unimore.it (S.C.); marco.manfredini@unimore.it (M.M.); caterina.longo@unimore.it (C.L.); giovanni.pellacani@unimore.it (G.P.)
- ² Morphological Sciences, Department of Surgical, Medical, Dental and Morphological Sciences Related to Transplant, Oncology and Regenerative Medicine, University of Modena and Reggio Emilia, 41125 Modena, Italy; laura.bertoni@unimore.it
- ³ Department of Surgical and Morphological Sciences, University of Insubria, 21100 Varese, Italy; nicola.zerbinati@uninsubria.it
- ⁴ Centro Oncologico ad Alta Tecnologia Diagnostica-Dermatologia, Azienda Unità Sanitaria Locale-IRCCS di Reggio Emilia, 42123 Reggio Emilia, Italy
- ⁵ Dermatology Clinic, Department of Clinical Internal, Anesthesiological and Cardiovascular Sciences, Sapienza University of Rome, 00161 Rome, Italy
- * Correspondence: stefania.guida@unimore.it; Tel.: +39-0594222464; Fax: +39-0594224363



Citation: Guida, S.; Arginelli, F.; Farnetani, F.; Ciardo, S.; Bertoni, L.; Manfredini, M.; Zerbinati, N.; Longo, C.; Pellacani, G. Clinical Applications of In Vivo and Ex Vivo Confocal Microscopy. *Appl. Sci.* **2021**, *11*, 1979. <https://doi.org/10.3390/app11051979>

Academic Editor: Stefano Selci

Received: 30 January 2021

Accepted: 19 February 2021

Published: 24 February 2021

Publisher's Note: MDPI stays neutral with regard to jurisdictional claims in published maps and institutional affiliations.



Copyright: © 2021 by the authors. Licensee MDPI, Basel, Switzerland. This article is an open access article distributed under the terms and conditions of the Creative Commons Attribution (CC BY) license (<https://creativecommons.org/licenses/by/4.0/>).

Abstract: Confocal laser scanning microscopy (CLSM) has been introduced in clinical settings as a tool enabling a quasi-histologic view of a given tissue, without performing a biopsy. It has been applied to many fields of medicine mainly to the skin and to the analysis of skin cancers for both in vivo and ex vivo CLSM. In vivo CLSM involves reflectance mode, which is based on refractive index of cell structures serving as endogenous chromophores, reaching a depth of exploration of 200 µm. It has been proven to increase the diagnostic accuracy of skin cancers, both melanoma and non-melanoma. While histopathologic examination is the gold standard for diagnosis, in vivo CLSM alone and in addition to dermoscopy, contributes to the reduction of the number of excised lesions to exclude a melanoma, and to improve margin recognition in lentigo maligna, enabling tissue sparing for excisions. Ex vivo CLSM can be performed in reflectance and fluorescent mode. Fluorescence confocal microscopy is applied for “real-time” pathological examination of freshly excised specimens for diagnostic purposes and for the evaluation of margin clearance after excision in Mohs surgery. Further prospective interventional studies using CLSM might contribute to increase the knowledge about its application, reproducing real-life settings.

Keywords: skin cancer; in vivo confocal microscopy; ex vivo confocal microscopy; melanoma; basal cell carcinoma

1. Introduction

In the last few decades, confocal laser scanning microscopy (CLSM), also known as confocal microscopy, has been used in clinical practice as a tool enabling a quasi-histologic resolution of a given tissue in a few minutes. CLSM has been employed in different fields of medicine, such as dermatology, as a non-invasive technique to visualize different skin layers at a high-resolution and it has been proven as an add-tool for the identification of skin cancers, though histopathology represents the gold standard for diagnosing skin tumors [1–3].

The technique, involving light collection from the “in focus” plane through a pinhole, was firstly described by Marvin Minsky in 1955, but it was in 1990s that Rajadhyaksha et al.

first conceived reflectance confocal microscopy (RCM) as a device in skin imaging, thanks to progressive advances in instrument development [4,5].

Confocal microscopes can be used with two different modalities: *in vivo* and *ex vivo*.

The first one is applied for *in vivo* exploration of tissues that can be reached directly such as the eyes, skin and mucosae or indirectly, through endomicroscopy, such as gastrointestinal and genitourinary tract, for lung and in intraoperative brain tumor imaging with the aim of a diagnosis with a quasi-histological resolution without any biopsy [6,7].

In vivo CLSM involves reflectance mode (reflectance confocal microscopy, RCM), exploiting backscattered light from cell structures, which is based on refractive index of cell structures and organelles, with keratin, melanin and collagen showing higher refractive indices compared to water, therefore serving as “endogenous chromophores” [5].

Ex vivo CLSM can be performed in reflectance and fluorescent mode. Fluorescence confocal microscopy (FCM) is usually employed, enabling the visualization of cellular details through fluorescent agents to produce image contrast. FCM is applied for “real-time” pathological examination of freshly excised specimens for diagnostic purposes and for the evaluation of margin clearance after excision [7–10].

The aim of this review is to present current clinical applications of CLSM, both *in vivo* and *ex vivo*, focusing mainly on skin applications.

2. In Vivo Confocal Laser Scanning Microscopy

RCM represents a non-invasive imaging technique permitting the observation at a quasi-histological resolution of a given tissue, *in vivo*, therefore avoiding a biopsy. When applied to the skin, RCM enables the exploration of different layers including epidermis, dermo-epidermal junction (DEJ) and upper dermis, reaching up to 200 µm of depth, therefore impairing both the visualization of the deepest part of dermis and the evaluation of the thickness of lesions [6,7]. However, despite this limitation, the high-resolution and the visualization of gray-scale horizontal images of cells and nuclear structures at epidermal level, collagen, and circulating blood cells at dermal layer, enable the identification of clues for diagnosis of different skin conditions. Among these, an increased diagnostic accuracy of melanocytic and nonmelanocytic skin lesions has been described, as well as an improved recognition of variations related to pigmentary disorders, inflammatory skin diseases and skin aging features [11].

Technically, *in vivo* RCM has a lateral resolution of 0.5–1 µm and an axial of 3–4 µm. A schematic representation of optical principals of CLSM is reported in Figure 1.

The acquisition of images with *in vivo* CLSM can be performed with skin-contact devices, the wide-probe (Vivascope 1500[®], MAVIG GmbH, Munich, Germany) and the handheld RCM (Vivascope 3000[®], MAVIG GmbH, Munich, Germany). The first one allows the collection of mosaics (Vivablock) at three different layers including epidermis, DEJ and dermis, overlapping with the dermoscopic image through the Vivacam[®] (MAVIG GmbH, Munich, Germany), with a maximum size of 8 × 8 mm, while the latter permits the evaluation of difficult-to-access areas of the head such as the nose, the eyelids and ears, the scalp and mucosae such as the nose, ears, eyelids, scalp and mucosae [12–14]. Main applications of *in vivo* CLSM are summarized in Table 1.

2.1. Diagnostic Accuracy of Skin Cancers

RCM has been proven to increase diagnostic accuracy and improve the early identification of skin cancers and differentiation of equivocal melanocytic and non-melanocytic lesions [15–19]. However, histopathology is considered the gold standard for the diagnosis of skin cancers.

Abbreviations: CLSM, confocal laser scanning microscopy; BCC, basal cell carcinoma; SCC, squamous cell carcinoma; LM/MM, lentigo maligna/lentigo maligna melanoma. # through endomicroscopy.

The improved diagnostic accuracy related to RCM has an impact in the reduction of the number of lesions excised to exclude a melanoma, the number needed to excise

(NNE). Accordingly, the NNE with dermoscopy has been estimated between 8.7 and 29.4 with dermoscopy and between 2.4 and 6.8 after RCM analysis [3,20,21]. Going into details of diagnostic accuracy obtained with RCM, a recent meta-analysis highlighted a pooled sensitivity of 92% and a 70% specificity of RCM for melanoma diagnosis on a total of 7352 lesions [22]. Similar results were obtained using a combined approach of dermoscopy and RCM in a subset of at-risk patients showing multiple atypical nevi [23].

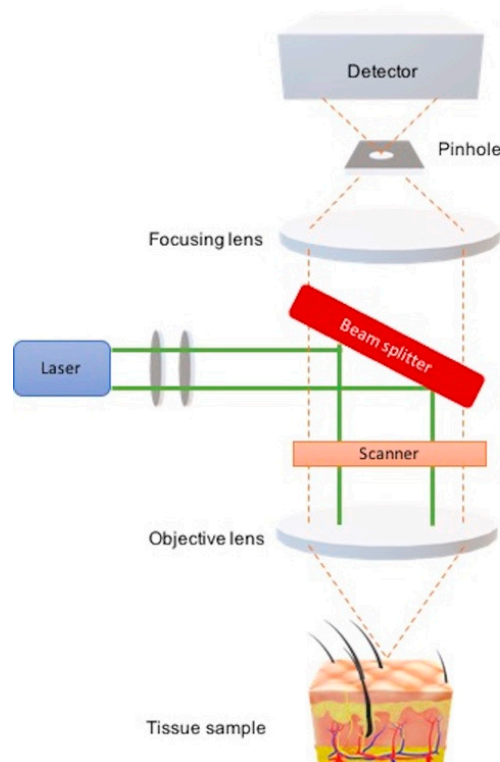


Figure 1. Schematic representation of optical principles of confocal laser scanning microscopy.

Variations of specificity were observed, showing an increased specificity for studies including consecutive lesions, and a lower specificity for prospective interventional studies. Interestingly, RCM specificity for malignant melanoma was found to be superior to dermoscopy, reaching 56% vs. 38%, respectively [22]. A Cochrane meta-analysis focusing on keratinocytic skin cancers, revealed a sensitivity of 94–95% and a specificity of 85–95% for RCM diagnosis of basal cell carcinoma (BCC) in patients showing equivocal lesions, while the sensitivity seems to be lower when including any suspicious lesion (sensitivity 76–95; specificity 95%) [18].

Interestingly, the diagnostic accuracy of RCM is lower as compared to that obtained when clinical, dermoscopic and RCM data are available [24]. However, this trend has been shown also with histopathology [25]. Moreover, the accuracy of diagnosis has been related to the experience of RCM readers. In recent prospective study, involving 1279 consecutive equivocal skin lesions sent for RCM consultation, experienced RCM readers reached a 95% sensitivity and 83.9% specificity [3]. A reduced sensitivity and specificity for recent RCM users in the diagnosis of malignant versus benign lesions was observed (mean sensitivity 88.9%; mean specificity 79.3%) [26].

However, when defining four main RCM features for the identification for skin cancers, with two melanoma-specific key features (atypical cells and DEJ disarray), one for BCC (basaloid cords/islands), and one for SCC (keratinocyte disarray), recent RCM users reached an overall sensitivity for the diagnosis of skin cancer of 91%, higher for melanoma (93%) and BCC (92%), and lower for SCC (67%), and an overall specificity of 57% [1].

In daily practice, some indications have been described as highly amenable for *in vivo* RCM such as flat pigmented lesions on sun-damaged skin and non-pigmented lesions of the face. On the contrary, nodular and/or hyperkeratotic lesions should be analyzed with caution, as well as conditions with discrepancy between clinic and dermoscopic appearance and RCM features [27,28].

2.2. Main *In Vivo* CLSM Diagnostic Clues in Skin Cancers

The incidence of skin cancers is rising throughout the world, with cutaneous melanoma being associated with 90% mortality related to skin malignancies. Melanoma prognosis is dependent on Breslow index, with increased thickness being associated with worse outcomes and lower survival rates [29]. Thus, an early diagnosis, supported by non-invasive skin imaging techniques, has a pivotal role [13,30–32].

As previously mentioned, two melanoma-specific RCM key-features, represented by “atypical cells” and “dermal-epidermal junction disarray”, have been described [1]. These features are basically shared by all melanoma type included lentigo maligna/lentigo maligna melanoma (LM/LMM), superficial spreading (SSM) and nodular melanoma (NM).

LM and LMM are mainly located on the face and other photo-exposed skin sites. RCM contributes to LM/LMM diagnosis through the identification of a disarranged epidermis and atypical cells (cells with atypia in terms of shape and size) at epidermal layer or infiltrating the hair follicle and a meshwork pattern with melanocytes aggregates (nests) at the DEJ [33]. In addition, the “medusahead-like” feature, showing elongated buddings bulging from the hair follicle and filled with atypical cells (with dendritic or pleomorphic appearance), represents another important diagnostic clue for LM/LMM [34], as well as folliculotropism [35]. Interestingly, the identification of melanocytic nests with RCM, contribute to the differential diagnosis with other pigmented macules of the face [36].

To date, superficial spreading melanoma (SSM) represents the most common form of melanoma in Caucasians while NM is less represented [37,38]. RCM variations corresponding to changes in each skin layer can be observed and a melanoma classification according to RCM features, corresponding to different molecular alterations, has been established [39,40].

The prevalence of atypical cells with dendritic shape (above all in “solar” melanoma which develops in patients with low nevus count and sun-damaged skin) is observed in type 1 melanoma [14,39], while roundish cells (above all in melanomas in subjects with numerous nevi and a history of intermittent sun exposure), as well as non-edged papillae at DEJ [39,41], are typical of type 2 (Figure 2a,b). With increasing thickness of SSM, and also in some NMs, an increased degree of disarrangement within epidermis, cell pleomorphism, and melanocytic nests, organized in a cerebriform fashion, progressively infiltrating dermal papillae can be also observed (type 3) [39,42] (Figure 2c,d). An additional feature of thick melanomas is represented by dark areas with irregular contours and sharp borders, containing amorphous material, corresponding to ulceration [43]. Furthermore, a combination of atypical cells with dendritic and roundish appearance has been described in type 4 melanomas [39].

Interestingly, RCM characteristics of melanoma metastasis have been described and they have been found to correlate with dermatropic and epidermotropic diagnoses with histopathology [44].

Non-melanoma skin cancers (NMSCs), including BCC and actinic keratosis/squamous cell carcinoma (AK/SCC), are the most common malignancy in populations with fair skin and intermittent or chronic exposure to UV radiation [45].

BCC is the most frequent skin tumor, characterized by local invasion, while about 20% is represented by SCC, with a worst prognosis related to the risk of potential metastatization [13]. BCC is typified by basaloid cords and or tumor islands with RCM [1]. Tumor islands are composed by highly packed cells with high refractivity and polarization, surrounded by clefting, corresponding to dark spaces around tumor nests [46] (Figure 3a,b). Other peculiar findings in BCCs are abundant inflammatory infiltrate (visible as

bright cells with irregular contours and without nucleus, also known as melanophages) distributed inside and outside the tumor islands, increased number of dilated blood vessels [47]. Furthermore, different features can be observed in BCC depending on the degree of pigmentation. Pigmented BCC may show dendritic cells, corresponding to melanocytes inside the tumor island [48,49], while non-pigmented BCC is characterized by dark silhouettes, defined as areas with hyporeflexivity, corresponding to basaloid islands, outlined by bright collagen bundles in the surrounding dermis [48,50]. The “epidermal shadowing” corresponds to large dark featureless areas creating a disruption of the epidermis in relation to clefting of the underlying tumor nests [46]. Additionally, RCM contributes to the recognition of criteria corresponding to different BCC subtypes [51], with an impact on treatment choice.

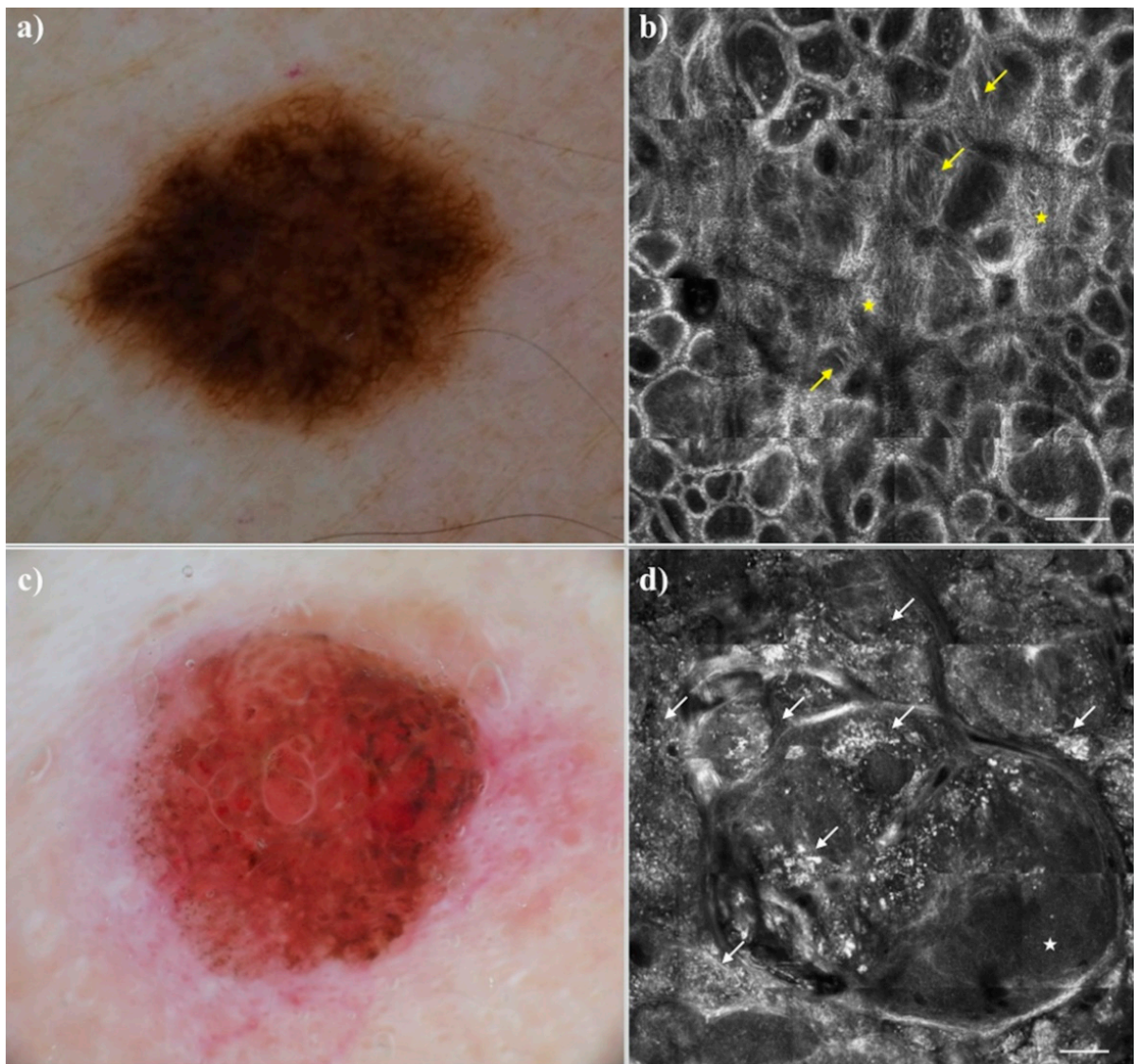


Figure 2. (a) Dermoscopy of a melanoma in situ. (b) In vivo reflectance confocal microscopy showing several pagetoid cells (yellow stars) at the epidermal level and atypical cells at dermo-epidermal junction (yellow arrows). Scale bar 200 μm . (c) Dermoscopy of a melanoma, 5.3 mm Breslow thickness. (d) In vivo reflectance confocal microscopy showing atypical melanocytes (white arrows), predominantly organized in nests and cerebriform nests (white star). Scale bar 200 μm .

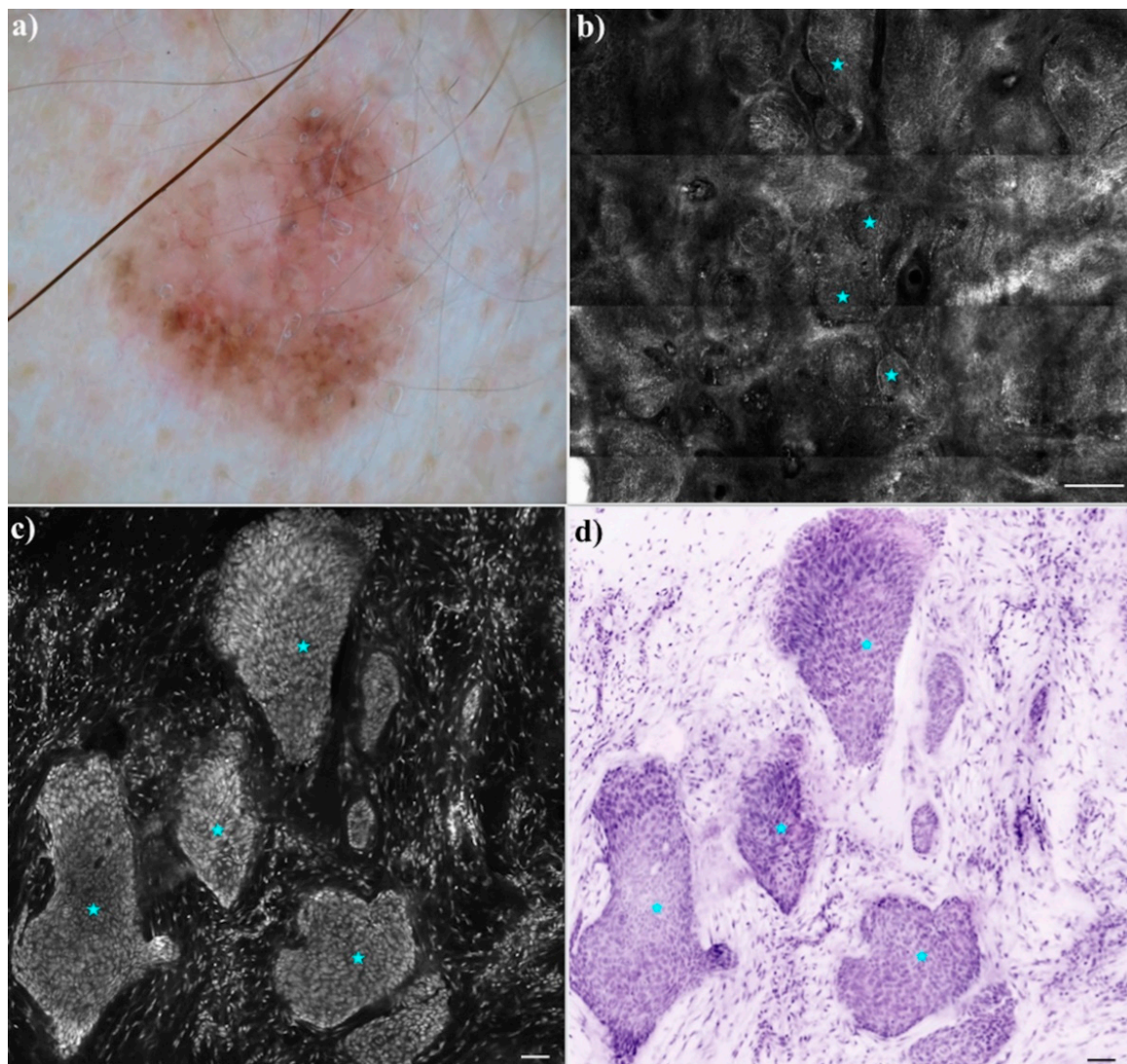


Figure 3. (a) Dermoscopy of a nodular basal cell carcinoma. (b) In vivo reflectance confocal microscopy showing tumor islands with palisading (blue arrows) and peripheral clefting in horizontal section. Scale bar 200 μm . (c) High-resolution fluorescence confocal microscopy image showing basaloid islands (blue arrows) with peripheral palisading and clefting that corresponded to the ones seen on hematoxylin & eosin digitally stained (d). Scale bar 200 μm .

AK/SCC are typified by disarranged or mildly atypical honeycomb pattern, with RCM [1]. Furthermore, in AK, nuclear retention, corresponding to parakeratosis in histology, is visualized as a dark round structure located in the middle of corneocytes. At the superficial dermis bundles of lace-like collagen can be observed [52]. Interestingly, RCM enables AK grading, depending on the amount of keratinocytic atypia, showing good interobserver correlation between RCM and histopathology, with consequent advantages in the choice of the best treatment and to monitor the response to AK therapy [53–55].

An increased keratinocyte atypia and architectural disorder are observed in SCC, as compared to AK. With RCM, Bowen disease, or in situ SCC, it shows atypical honeycomb pattern, disruption of the stratum corneum, S-shaped blood vessels, and targetoid cells while invasive SCC is characterized by dark areas with sharp and irregular contours, filled with amorphous material, corresponding to ulceration, architectural disarrangement, round or polygonal cells with speckled appearance and dark nucleus in epidermis and irregular dilated vessels [56–58]. Currently, in doubtful cases, the differential diagnosis between AK and SCC requires a skin biopsy.

2.3. Pre-Surgical Mapping

While an accurate analysis of melanocytic lesions encompasses the use of the wide-probe in order to explore the entire lesion, the handheld RCM device [59,60] is employed not only for diagnostic purposes in difficult-to-reach areas, but also for pre-surgical mapping of LM/LMM borders [61].

Indeed, the management of LM/LMM may be challenging for ill-defined margins, possible subclinical spread, and common localization of these lesions on areas with an aesthetic impact, such as the face. Therefore, the possibility to non-invasively explore and mapping lesions before surgery represents an advantage in terms of healthy tissue sparing, thus reducing the number of skin biopsies and in order to plan an adequate treatment of LM/LMM and counsel patients appropriately.

The most recent techniques for non-invasive pre-surgical mapping are the Radial Videomosaicking RCM [62] and the smart approach [33]. The first one consists of confocal exploration from the center of the lesion, going radially to the periphery, using adhesive paper rings for the definition of the margins while the latter employs small skin cuts are used for the same purpose, proceeding radially outward the identified segment by 2 mm intervals until an RCM-negative margin is observed [33,62]. A prospective study involving 72 patients performed a comparison of the subclinical extension of LM/LMM identified through RCM and histopathology, revealing an overall agreement of 85.9% between RCM margin assessment and final histopathology [63].

Studies including a lower number of cases have investigated the role of RCM for margins evaluation in BCCs [64,65].

2.4. Other Applications of *In Vivo* CLSM

In vivo CLSM can be employed for identification of specific clues and monitoring the effects of treatment in inflammatory/autoimmune/infectious skin diseases, such as psoriasis, skin aging and hydration, together with results of rejuvenation and scar treatments, skin pigmentation and related disorders, such as melasma and vitiligo [66–74].

Psoriasis is characterized by scales and vessels, both visible with RCM, with scales corresponding to hyperkeratosis, associated with an increased epidermal thickness (>60–80 μm), measured through the number of stacks from the top of the stratum corneum to the first cellulated epidermal layer [75].

The exploration with RCM at epidermal level enables the visualization of a regular/irregular honeycombed pattern or eventual pigmentation corresponding to mottled pigmentation while at DEJ/superficial dermis blood vessels and collagen can be observed [61]. Interestingly, variation in pigmentation and collagen remodeling, have been described after laser and rejuvenation treatments [68,70,74,76–80].

RCM has been used to study acne skin and different features corresponding to comedo, papules and pustules have been reported. Additionally, RCM has been applied to treatment monitoring, showing the reduction of both inflammatory and hyperkeratotic features with RCM [72,73,81].

2.5. Conclusions

In vivo CLSM enables the visualization with a cellular resolution of the skin. This technique has proven to increase the diagnostic accuracy of skin cancers in different clinical settings, therefore reducing the amount of unnecessary excisions, with higher levels of sensitivity and specificity for expert RCM readers as compared to novel users. However, the identification of four main skin cancer features enabled the increase in sensitivity for recent users. Similarly to histopathology, when employed with clinical and dermoscopic data, RCM has shown an improved diagnostic accuracy. Nevertheless, the high resolution of this non-invasive diagnostic technique is limited to a depth of up to 200 μm , therefore impairing the visualization of deeper layer of the dermis. However, data coming from further prospective interventional studies using *in vivo* CLSM might contribute to increase

the knowledge about its application, integrating clinical and dermoscopic information, reproducing real-life setting.

Moreover, RCM can be applied to other fields of Dermatology as well as to other fields of Medicine.

3. Ex Vivo Confocal Laser Scanning Microscopy

Ex vivo CLSM applied to skin analysis has been available on the market since 2013, so it is a relatively new and not fully explored imaging technique, allowing a real-time microscopic examination of freshly excised unfixed tissue, exploring structures and cells at a near histologic resolution. The analyzed specimen is optically sliced, scanned by a point source of light (laser) and, through a pinhole rejecting out of focus light, a thin section of tissue is obtained and displayed on a monitor [7,82].

To date, the only commercially available device is VivaScope 2500 (MAVIG GMBH, Munich, Germany), a new version of VivaScope 2000. Ex vivo CLSM works in two different modalities: the reflectance mode (830 nm laser wavelength), mainly employed for in vivo settings and the fluorescence mode (488 or 658 nm laser wavelength), usually employed for ex vivo examination [7,83].

Using reflectance mode, no staining is required, because the contrast is related to the different refractive index of cellular structures (i.e., melanin, keratin), similarly to in vivo RCM [83,84].

In 2001, Rajadhyaksha et al. reported the first pictures obtained from BCC excised during Mohs micrographic surgery, highlighting the necessity to improve the quality of images through a staining technique to enhance the contrast [8].

Fluorochromes in ex vivo CLSM act like dyes in histopathology, enabling the identification of cell and tissue structures, depending on the wavelength of the exciting light as well as the features of the target tissue [85]. Among these agents, acridine orange is the most largely used, followed by methylene or toluidine or Nile blue, fluorescein or Patent blue V [82].

Acridine orange has been introduced as a nuclear contrast agent, able to bind nuclear DNA, offering the best contrast into epithelial tissues without affecting subsequent frozen sections and formalin-fixed histopathology quality. Bini et al. [86] compared three different concentrations of acridine orange (0.1, 0.3 and 0.6 mM), reaching the optimum at 0.6 mM for 20 s, to enhance the contrast, minimizing artifacts in the dermis.

The specimen can be observed entirely “en face” to assess the horizontal extension, or transversally, as for conventional histology; the examination of large lesions is possible because the instrument can show wide mosaics reaching up to 20×20 mm [87]. The tissue sample is embedded between two glass slides fixed together with silicon glue, enabling both sides examination. Aqueous gel or silicone can be applied in order to aid the contact of the external part of the sample and the glass slide. Furthermore, obtaining a flattened sample, by means of a “tissue press”, is important to avoid potential artifacts resulting from an irregular contact between the surface of the specimen and the glass slide that may be related to irregular cutting. When put on the microscope stage, each specimen is scanned along the x-axis and the y-axis using a diode laser illumination. A two-dimensional, high-resolution sequence of horizontal images of 750×750 μm of the different tissue layers up to a thickness of 200 μm is acquired and stitched together into a mosaic. The lateral and axial spatial resolutions are 1 μm and 3 μm , respectively. Since the microscope is confocal, only the in-focus plane can be visualized and it has to be adjusted moving the objective lens [82].

The displayed image depends on the conversion of the reflectant/fluorescent signal from nuclei of cells by a software. In reflectance mode, gray-scale images are visualized, showing dark hypo-reflective structures and bright hyper-reflective structures, overlapping to in vivo RCM appearance. On the other hand, with fluorescence contrast, non-fluorescent structures appear dark, as compared to the white fluorescent ones. In particular, cellular nuclei stained with acridine orange appear white, therefore enabling a better visualization

of keratinocytes, hair follicle epithelium, fibroblasts, sebaceous and eccrine glands and tumor cells. Consequently, the brightness of images is directly related to the amount of nuclei in the tissue, with bright images obtained in lymph nodes or in tumors, and a dark background in hypocellular samples such as in fibrous or in adipose tissue showing a low-to-absent fluorescent signal. Despite the limitation due to the low fluorescent signal, ex vivo CLSM enables the study of muscles and adipose tissue, with the combination of both reflectance and fluorescence modes [7,88].

Gareau et al. reported the digital purple and pink stain of confocal mosaics in order to simulate pathology images appearance, in order to improve the recognition of structures, adapting FCM images to those of hematoxylin and eosin (H&E) stain [89]. When nuclei are stained with acridine orange, they are imaged in exogenous fluorescent mode while cell cytoplasm and dermis are visualized through reflectance contrast. After that, fluorescence mosaics can be digitally stained purple (mimicking hematoxylin), whereas reflectance mosaics can be digitally stained pink (mimicking eosin). The final result is a mosaic similar to histology [86,89,90]. Overall, different image visualizations are available including separate or combined reflectance/fluorescence and H&E-like modes.

The most employed application of FCM is the intraoperative assessment of tumor margins during Mohs surgery for the removal of BCC [91–93]. However, FCM use has been extended to other skin tumors, such as SCC and melanoma [82], healthy skin [94], nails and hair diseases [95,96], diagnosis of skin infections (viral and superficial/deep fungal infections) [97], mucosa diseases [95,98], inflammatory disease [99] and aesthetic medicine [100–102]. Main applications of ex vivo CLSM are summarized in Table 1.

3.1. Main Ex Vivo CLSM Clues of Skin Cancer and Inflammatory Skin Diseases

As previously mentioned, the most employed application of FCM is represented by margin definition of BCCs during Mohs surgery.

Ex vivo CLSM allows a quick evaluation of surgical skin samples, directly in the surgical room. Therefore, this technique represents a potential replacement of intraoperative histology for tumor margins assessment on frozen tissues during Mohs surgery. Mosaics are generally created and interpreted in 10 min, while the preparation of cryopreserved sections for histopathologic examination may require 20 to 45 min per excision, becoming time and cost consuming during daily clinical practice [7,8].

One of the limitations of ex vivo CLSM seems to be related to the poor ability to differentiate cytological and architectural details. Accordingly, a specific staining cannot distinguish between different cell types, although the use of fluorescent-labelled specific antibodies may overcome this problem [103–105].

Similarly to RCM, FCM shows areas of high fluorescence organized to form structures/aggregates in contrast with the surrounding hyporeflective stroma or cells agglomerate, corresponding to tumor islands, with peripheral palisading, in BCCs. These structures are surrounded by hypofluorescent dark-appearing space, corresponding to clefting which is typical of superficial and nodular BCCs and less demarcated in infiltrative ones [83,106].

Additionally, other BCC features are represented by nuclear pleomorphism visualized as a variation of nuclear shape and/or increased nucleus/cytoplasm ratio and modified stroma surrounding the BCC nests, showing a dark background with fluorescent dots and filaments that correspond to fibroblasts, collagen fibers, and inflammatory infiltrate [83,106]. Bennassar et al. reported that FCM had an overall sensitivity of 88% and specificity of 99% in detecting residual BCC, on a sample of 69 BCCs [106]. Similar results were obtained in a prospective study by Longo et al. on a sample of 753 BCCs [107].

FCM enables the identification of different features in diverse BCC subtypes, with proliferation of atypical basaloid cells forming an axis parallel to the epidermal surface and cleft-like spaces typically described in superficial BCCs and nodules with peripheral palisading and clefting in nodular BCCs (Figure 3c,d). Infiltrative BCC is the most challenging subtype, formed by columns and cords of basaloid cells mixed with a collagenic stroma [83,84,108].

FCM has also been applied to margin assessment in SCC [109,110]. A total of 41 out of 43 margins in 13 SCC were positive in both FCM and histopathology, therefore providing a good correlation between the two evaluations. In detail, confocal criteria for the diagnosis and evaluation of the degree of differentiation have been described, such as well-defined tumor silhouette, presence of numerous low fluorescent keratin pearls, keratin formation corresponding to fluorescent scales in well differentiated SCC and marked nuclear pleomorphism in poorly differentiated tumors [109].

Interestingly, a recent experience of margin assessment in LM/LMM with ex vivo CLSM has been reported in the literature, demonstrating a good rate of correct margins identification for LM/LMM (95.2%). In this study, the authors combined in vivo preoperative analysis an ex vivo one, a promising approach for mucosal melanoma, LM and LMM, especially when aesthetically or functional relevant areas are involved, in order to avoid staged excision [87].

A preliminary study on inflammatory skin diseases with FCM was performed by Bertoni et al. with the aim to verify the correspondence between histologic images and confocal ones. Despite limitations related to manual sectioning of the specimen, this study showed an encouraging percentage of correct diagnosis. Psoriasis, in particular had the highest reliability (90.5%), while eczema showed the least reliability [99]. Recently, Mentzel et al. showed that skin features such as epidermal alterations, including hyperkeratosis, parakeratosis and spongiosis, as well as variations at dermal level, like fibrosis or vascular variations can be clearly visualized with ex vivo CLSM [111].

The future purpose of ex vivo CLSM is to fill the time frame that separates the biopsy from diagnosis and therefore from therapy [99].

3.2. Applications in Organs Other than the Skin

The first study applying ex vivo FCM on different surgical specimens other than skin, was published by Ragazzi et al. in the 2014. In this pilot study the principal aim was to generate images from the tissue explored, to compare them with the histological ones [89].

Krishnamurthy et al. and Ragazzi et al. evaluated and reviewed the application of ex vivo CLSM for breast, genitourinary tract, gastrointestinal tract and liver, thyroid and parathyroid, lymph nodes and larynx and lungs [7,88,112].

Additionally, a promising, simple and quick (less than 5 min for specimen) application is represented by prostate cancer. Prostatic acinar adenocarcinoma is typified with FCM by nuclear atypia, irregular morphology of the glands, prominent nucleolus and absence of basal cell layers [113,114].

A substantial level of agreement between FCM and histology has been proven on 89 specimens collected from 13 patients undergoing radical laparoscopic prostatectomy for malignancy, with FCM showing a sensitivity of 83.3%, a specificity reaching 93.5% and 91% diagnostic accuracy, as compared to conventional histology [113].

3.3. Conclusions

Ex vivo CLSM offers a real-time examination of the excised tissue in reflectance and fluorescence modes, enabling also the application of fluorescent-labelled antibodies. Reflectance and fluorescence ex vivo CLSM, along with H&E-like digital staining images, show to be promising in different clinical fields, especially skin pathology.

In conclusion, ex vivo CLSM is a novel imaging diagnostic tool enabling the analysis of tissue sample of a diameter of 2 cm. Thin sections of surgical samples are not required for the examination. Currently, the main clinical application is represented by skin tumor margin assessment in BCC and promising results have been obtained in the analysis of prostate cancer. Additionally, ex vivo CLSM features of cancers such as SCC, LM and others as well as skin inflammatory disorders have been preliminary explored, thus representing potential fields of application in the future.

However, the use of ex vivo CLSM is limited by the high cost of the tool as well as by the learning curve for the image readers. However, ex vivo CLSM has proven to

be a reliable and reproducible technique as compared to histopathology, especially in dermatologic and urologic applications.

Table 1. Main applications of in vivo and ex vivo confocal laser scanning microscopy.

In Vivo CLSM		
Skin	Specific applications for the skin:	Principal references:
	Melanocytic and non-melanocytic lesions diagnosis and monitoring	[1,5,11,12,16,18–20,22,39,46]
	Pre-surgical mapping	[33,60,62–64]
	Diagnosis and monitoring of inflammatory/autoimmune/infectious and pigmentary skin disorders	[66–68,72,75]
	Aging and related applications	[69,74–76]
Hair and nails		
Mucosae and conjunctiva		
Eyes		
Genitourinary tract #		
Gastrointestinal tract #		
Lung #		
Brain #		
Ex vivo CLSM		
Skin	Main application for the skin:	Principal references:
	BCC diagnosis and margin definition	[9,83,84,92,93,108]
	Other applications:	
	SCC and LM/LMM diagnosis and margin definition	[87,109]
	Inflammatory/autoimmune/infectious skin diseases	[97,99,111]
Aging and related applications	[100,102]	
Nail		
Mucosae		
Prostate and other parts of the genitourinary tract		
Breast		
Thyroid and parathyroid		
Larynx and lung		
Lymph nodes		
Gastrointestinal tract and liver		

Author Contributions: Conceptualization, G.P. and S.G.; validation, C.L.; resources, S.C., L.B.; writing—original draft preparation, S.G., F.A.; writing—review and editing, M.M., F.F.; visualization, N.Z.; supervision, G.P. All authors have read and agreed to the published version of the manuscript.

Funding: This research received no external funding.

Institutional Review Board Statement: Not applicable.

Informed Consent Statement: Not applicable.

Conflicts of Interest: The authors declare no conflict of interest.

References

- Pellacani, G.; Scope, A.; Gonzalez, S.; Guitera, P.; Farnetani, F.; Malvehy, J.; Witkowski, A.; De Carvalho, N.; Lupi, O.; Longo, C. Reflectance confocal microscopy made easy: The 4 must-know key features for the diagnosis of melanoma and nonmelanoma skin cancers. *J. Am. Acad. Dermatol.* **2019**, *81*, 520–526. [[CrossRef](#)] [[PubMed](#)]
- Yélamos, O.; Manubens, E.; Jain, M.; Chavez-Bourgeois, M.; Pulijal, S.V.; Dusza, S.W.; Marchetti, M.A.; Barreiro, A.; Marino, M.L.; Malvehy, J.; et al. Improvement of diagnostic confidence and management of equivocal skin lesions by integration of reflectance confocal microscopy in daily practice: Prospective study in 2 referral skin cancer centers. *J. Am. Acad. Dermatol.* **2020**, *83*, 1057–1063. [[CrossRef](#)]

3. Borsari, S.; Pampena, R.; Lallas, A.; Kyrgidis, A.; Moscarella, E.; Benati, E.; Raucci, M.; Pellacani, G.; Zalaudek, I.; Argenziano, G.; et al. Clinical Indications for Use of Reflectance Confocal Microscopy for Skin Cancer Diagnosis. *JAMA Dermatol.* **2016**, *152*, 1093–1098. [[CrossRef](#)]
4. Minsky, M. Memoir on inventing the confocal scanning microscope. *Scanning* **1988**, *10*, 128–138. [[CrossRef](#)]
5. Rajadhyaksha, M.; Grossman, M.; Esterowitz, D.; Webb, R.H.; Anderson, R.R. In Vivo Confocal Scanning Laser Microscopy of Human Skin: Melanin Provides Strong Contrast. *J. Investig. Dermatol.* **1995**, *104*, 946–952. [[CrossRef](#)]
6. Kiesslich, R.; Goetz, M.; Vieth, M.; Galle, P.R.; Neurath, M.F. Confocal Laser Endomicroscopy. *Gastrointest. Endosc. Clin. N. Am.* **2005**, *15*, 715–731. [[CrossRef](#)]
7. Ragazzi, M.; Longo, C.; Piana, S. Ex Vivo (Fluorescence) Confocal Microscopy in Surgical Pathology: State of the Art. *Adv. Anat. Pathol.* **2016**, *23*, 159–169. [[CrossRef](#)]
8. Rajadhyaksha, M.; Menaker, G.; Flotte, T.; Dwyer, P.J.; Gonzalez, S.; Gonz, S. Confocal Examination of Nonmelanoma Cancers in Thick Skin Excisions to Potentially Guide Mohs Micrographic Surgery Without Frozen Histopathology. *J. Investig. Dermatol.* **2001**, *117*, 1137–1143. [[CrossRef](#)] [[PubMed](#)]
9. Chung, V.Q.; Dwyer, P.J.; Nehal, K.S.; Rajadhyaksha, M.; Menaker, G.M.; Charles, C.; Jiang, S.B. Use of Ex Vivo Confocal Scanning Laser Microscopy during Mohs Surgery for Nonmelanoma Skin Cancers. *Dermatol. Surg.* **2004**, *30*, 1470–1478. [[CrossRef](#)]
10. Patel, Y.G.; Nehal, K.S.; Aranda, I.; Li, Y.; Halpern, A.C.; Rajadhyaksha, M. Confocal reflectance mosaicing of basal cell carcinomas in Mohs surgical skin excisions. *J. Biomed. Opt.* **2007**, *12*, 034027. [[CrossRef](#)] [[PubMed](#)]
11. Rajadhyaksha, M.; González, S.; Zavislan, J.M.; Anderson, R.R.; Webb, R.H. In Vivo Confocal Scanning Laser Microscopy of Human Skin II: Advances in Instrumentation and Comparison with Histology. The authors have declared conflict of interest. *J. Investig. Dermatol.* **1999**, *113*, 293–303. [[CrossRef](#)] [[PubMed](#)]
12. Pellacani, G.; Guitera, P.; Longo, C.; Avramidis, M.; Seidenari, S.; Menzies, S. The Impact of In Vivo Reflectance Confocal Microscopy for the Diagnostic Accuracy of Melanoma and Equivocal Melanocytic Lesions. *J. Investig. Dermatol.* **2007**, *127*, 2759–2765. [[CrossRef](#)] [[PubMed](#)]
13. Guida, S.; De Pace, B.; Ciardo, S.; Farnetani, F.; Pellacani, G. Non-invasive Imaging for Skin Cancers—the European Experience. *Curr. Dermatol. Rep.* **2019**, *8*, 172–181. [[CrossRef](#)]
14. Guida, S.; Longo, C.; Casari, A.; Ciardo, S.; Manfredini, M.; Reggiani, C.; Pellacani, G.; Farnetani, F. Update on the use of confocal microscopy in melanoma and non-melanoma skin cancer. *G. Ital. Dermatol. Venereol.* **2015**, *150*, 547–563. [[PubMed](#)]
15. Pellacani, G.; Cesinaro, A.M.; Seidenari, S. Reflectance-mode confocal microscopy of pigmented skin lesions—improvement in melanoma diagnostic specificity. *J. Am. Acad. Dermatol.* **2005**, *53*, 979–985. [[CrossRef](#)]
16. Guitera, P.; Menzies, S.W.; Longo, C.; Cesinaro, A.M.; Scolyer, R.A.; Pellacani, G. In Vivo Confocal Microscopy for Diagnosis of Melanoma and Basal Cell Carcinoma Using a Two-Step Method: Analysis of 710 Consecutive Clinically Equivocal Cases. *J. Investig. Dermatol.* **2012**, *132*, 2386–2394. [[CrossRef](#)]
17. Lovatto, L.; Carrera, C.; Salerni, G.; Alós, L.; Malvehy, J.; Puig, S. In vivo reflectance confocal microscopy of equivocal melanocytic lesions detected by digital dermoscopy follow-up. *J. Eur. Acad. Dermatol. Venereol.* **2015**, *29*, 1918–1925. [[CrossRef](#)] [[PubMed](#)]
18. Dinnes, J.; Deeks, J.J.; Chuchu, N.; Saleh, D.; Bayliss, S.E.; Takwoingi, Y.; Davenport, C.; Patel, L.; Matin, R.N.; O’Sullivan, C.; et al. Reflectance confocal microscopy for diagnosing keratinocyte skin cancers in adults. *Cochrane Database Syst. Rev.* **2018**, *12*, CD013191. [[CrossRef](#)]
19. Dinnes, J.; Deeks, J.J.; Saleh, D.; Chuchu, N.; Bayliss, S.; Patel, L.; Davenport, C.; Takwoingi, Y.; Godfrey, K.; Matin, R.N.; et al. Reflectance confocal microscopy for diagnosing cutaneous melanoma in adults. *Cochrane Database Syst. Rev.* **2018**, *12*, 013190. [[CrossRef](#)] [[PubMed](#)]
20. Pellacani, G.; Pepe, P.; Casari, A.; Longo, C. Reflectance confocal microscopy as a second-level examination in skin oncology improves diagnostic accuracy and saves unnecessary excisions: A longitudinal prospective study. *Br. J. Dermatol.* **2014**, *171*, 1044–1051. [[CrossRef](#)]
21. Alarcon, I.; Carrera, C.; Palou, J.; Alos, L.; Malvehy, J.; Puig, S. Impact of in vivo reflectance confocal microscopy on the number needed to treat melanoma in doubtful lesions. *Br. J. Dermatol.* **2014**, *170*, 802–808. [[CrossRef](#)] [[PubMed](#)]
22. Pezzini, C.; Kaleci, S.; Chester, J.; Farnetani, F.; Longo, C.; Pellacani, G. Reflectance confocal microscopy diagnostic accuracy for malignant melanoma in different clinical settings: Systematic review and meta-analysis. *J. Eur. Acad. Dermatol. Venereol.* **2020**, *34*, 2268–2279. [[CrossRef](#)] [[PubMed](#)]
23. Longhitano, S.; Pampena, R.; Guida, S.; De Pace, B.; Ciardo, S.; Chester, J.; Longo, C.; Farnetani, F.; Pellacani, G. In vivo confocal microscopy: The role of comparative approach in patients with multiple atypical nevi. *Exp. Dermatol.* **2020**, *29*, 945–952. [[CrossRef](#)] [[PubMed](#)]
24. Scope, A.; Dusza, S.; Pellacani, G.; Gill, M.; Gonzalez, S.; Marchetti, M.; Rabinovitz, H.; Marghoob, A.; Alessi-Fox, C.; Halpern, A. Accuracy of tele-consultation on management decisions of lesions suspect for melanoma using reflectance confocal microscopy as a stand-alone diagnostic tool. *J. Eur. Acad. Dermatol. Venereol.* **2018**, *33*, 439–446. [[CrossRef](#)]
25. Ferrara, G.; Argenyi, Z.; Argenziano, G.; Cerio, R.; Cerroni, L.; Di Blasi, A.; Feudale, E.A.A.; Giorgio, C.M.; Massone, C.; Nappi, O.; et al. The Influence of Clinical Information in the Histopathologic Diagnosis of Melanocytic Skin Neoplasms. *PLoS ONE* **2009**, *4*, e5375. [[CrossRef](#)]

26. Farnetani, F.; Scope, A.; Braun, R.P.; Gonzalez, S.; Guitera, P.; Malvey, J.; Manfredini, M.; Marghoob, A.A.; Moscarella, E.; Oliviero, M.; et al. Skin Cancer Diagnosis With Reflectance Confocal Microscopy: Reproducibility of feature recognition and accuracy of diagnosis. *JAMA Dermatol.* **2015**, *151*, 1075–1080. [[CrossRef](#)]
27. Shahriari, N.; Grant-Kels, J.M.; Rabinovitz, H.; Oliviero, M.; Scope, A. Reflectance confocal microscopy: Principles, basic terminology, clinical indications, limitations, and practical considerations. *J. Am. Acad. Dermatol.* **2021**, *84*, 1–14. [[CrossRef](#)]
28. Rajadhyaksha, M.; Marghoob, A.; Rossi, A.; Halpern, A.C.; Nehal, K.S. Reflectance confocal microscopy of skin in vivo: From bench to bedside. *Lasers Surg. Med.* **2017**, *49*, 7–19. [[CrossRef](#)]
29. Garbe, C.; Amaral, T.; Peris, K.; Hauschild, A.; Arenberger, P.; Bastholt, L.; Bataille, V.; Del Marmol, V.; Dréno, B.; Fargnoli, M.C.; et al. European consensus-based interdisciplinary guideline for melanoma. Part 1: Diagnostics—Update 2019. *Eur. J. Cancer* **2020**, *126*, 141–158. [[CrossRef](#)] [[PubMed](#)]
30. Giuffrida, R.; Conforti, C.; Di Meo, N.; Deinlein, T.; Guida, S.; Zalaudek, I. Use of noninvasive imaging in the management of skin cancer. *Curr. Opin. Oncol.* **2020**, *32*, 98–105. [[CrossRef](#)]
31. Farnetani, F.; Scope, A.; Coco, V.; Guida, S.; Cesinaro, A.M.; Piana, S.; Peris, K.; Pellacani, G.; Longo, C. Paradigmatic cases of pigmented lesions: How to not miss melanoma. *J. Dermatol.* **2016**, *43*, 1433–1437. [[CrossRef](#)]
32. Agozzino, M.; Moscarella, E.; Babino, G.; Caccavale, S.; Piccolo, V.; Argenziano, G. The use of in vivo reflectance confocal microscopy for the diagnosis of melanoma. *Expert Rev. Anticancer. Ther.* **2019**, *19*, 413–421. [[CrossRef](#)]
33. Pellacani, G.; De Carvalho, N.; Ciardo, S.; Ferrari, B.; Cesinaro, A.; Farnetani, F.; Bassoli, S.; Guitera, P.; Star, P.; Rawson, R.; et al. The smart approach: Feasibility of lentigo maligna superficial margin assessment with hand-held reflectance confocal microscopy technology. *J. Eur. Acad. Dermatol. Venereol.* **2018**, *32*, 1687–1694. [[CrossRef](#)] [[PubMed](#)]
34. De Carvalho, N.; Farnetani, F.; Ciardo, S.; Ruini, C.; Witkowski, A.; Longo, C.; Argenziano, G.; Pellacani, G. Reflectance confocal microscopy correlates of dermoscopic patterns of facial lesions help to discriminate lentigo maligna from pigmented nonmelanocytic macules. *Br. J. Dermatol.* **2014**, *173*, 128–133. [[CrossRef](#)]
35. Persechino, F.; De Carvalho, N.; Ciardo, S.; De Pace, B.; Casari, A.; Chester, J.; Kaleci, S.; Stanganelli, I.; Longo, C.; Farnetani, F.; et al. Folliculotropism in pigmented facial macules: Differential diagnosis with reflectance confocal microscopy. *Exp. Dermatol.* **2018**, *27*, 227–232. [[CrossRef](#)] [[PubMed](#)]
36. Guida, S.; Farnetani, F.; De Pace, B.; Kaleci, S.; Chester, J.; Stanganelli, I.; Ciardo, S.; De Carvalho, N.; Longo, C.; Pellacani, G.; et al. Flat-pigmented facial lesions without highly specific melanocytic dermoscopy features: The role of dermoscopic globules and dots in differential diagnosis with corresponding reflectance confocal microscopy substrates. *J. Eur. Acad. Dermatol. Venereol.* **2019**, *34*, 153. [[CrossRef](#)] [[PubMed](#)]
37. Siegel, R.L.; Miller, K.D.; Jemal, A. Cancer statistics, 2019. *CA Cancer J. Clin.* **2019**, *69*, 7–34. [[CrossRef](#)]
38. Scope, A.; Zalaudek, I.; Ferrara, G.; Argenziano, G.; Braun, R.P.; Marghoob, A.A. Remodeling of the Dermoepidermal Junction in Superficial Spreading Melanoma: Insights gained from correlation of dermoscopy, reflectance confocal microscopy, and histopathologic analysis. *Arch. Dermatol.* **2008**, *144*, 1644–1649. [[CrossRef](#)]
39. Pellacani, G.; De Pace, B.; Reggiani, C.; Cesinaro, A.M.; Argenziano, G.; Zalaudek, I.; Soyer, H.P.; Longo, C. Distinct melanoma types based on reflectance confocal microscopy. *Exp. Dermatol.* **2014**, *23*, 414–418. [[CrossRef](#)]
40. Beretti, F.; Bertoni, L.; Farnetani, F.; Pellegrini, C.; Gorelli, G.; Cesinaro, A.M.; Bonetti, L.R.; Di Nardo, L.; Kaleci, S.; Chester, J.; et al. Melanoma types by in vivo reflectance confocal microscopy correlated with protein and molecular genetic alterations: A pilot study. *Exp. Dermatol.* **2019**, *28*, 254–260. [[CrossRef](#)] [[PubMed](#)]
41. Gareau, D.; Hennessy, R.; Wan, E.; Pellacani, G.; Jacques, S.L. Automated detection of malignant features in confocal microscopy on superficial spreading melanoma versus nevi. *J. Biomed. Opt.* **2010**, *15*, 061713. [[CrossRef](#)]
42. Pellacani, G.; Cesinaro, A.M.; Seidenari, S. In vivo assessment of melanocytic nests in nevi and melanomas by reflectance confocal microscopy. *Mod. Pathol.* **2005**, *18*, 469–474. [[CrossRef](#)] [[PubMed](#)]
43. Segura, S.; Pellacani, G.; Puig, S.; Longo, C.; Bassoli, S.; Guitera, P.; Palou, J.; Menzies, S.; Seidenari, S.; Malvey, J. In Vivo Microscopic Features of Nodular Melanomas: Dermoscopy, confocal microscopy, and histopathologic correlates. *Arch. Dermatol.* **2009**, *144*, 1311–1320. [[CrossRef](#)] [[PubMed](#)]
44. Farnetani, F.; Manfredini, M.; Longhitano, S.; Chester, J.; Shaniko, K.; Cinotti, E.; Mazzoni, L.; Venturini, M.; Manganoni, A.; Longo, C.; et al. Morphological classification of melanoma metastasis with reflectance confocal microscopy. *J. Eur. Acad. Dermatol. Venereol.* **2019**, *33*, 676–685. [[CrossRef](#)]
45. Ulrich, M.; Maltusch, A.; Rius-Diaz, F.; Röwert-Huber, J.; González, S.; Sterry, W.; Stockfleth, E.; Astner, S. Clinical Applicability of in vivo Reflectance Confocal Microscopy for the Diagnosis of Actinic Keratoses. *Dermatol. Surg.* **2008**, *34*, 610–619. [[CrossRef](#)]
46. Navarrete-Dechent, C.; DeRosa, A.P.; Longo, C.; Liopyris, K.; Oliviero, M.; Rabinovitz, H.; Marghoob, A.A.; Halpern, A.C.; Pellacani, G.; Scope, A.; et al. Reflectance confocal microscopy terminology glossary for nonmelanocytic skin lesions: A systematic review. *J. Am. Acad. Dermatol.* **2019**, *80*, 1414–1427. [[CrossRef](#)]
47. González, S.; Tannous, Z. Real-time, in vivo confocal reflectance microscopy of basal cell carcinoma. *J. Am. Acad. Dermatol.* **2002**, *47*, 869–874. [[CrossRef](#)] [[PubMed](#)]
48. Segura, S.; Puig, S.; Carrera, C.; Palou, J.; Malvey, J. Dendritic Cells in Pigmented Basal Cell Carcinoma: A relevant finding by reflectance mode confocal microscopy. *Arch. Dermatol.* **2007**, *143*, 883–886. [[CrossRef](#)]

49. Peccerillo, F.; Mandel, V.D.; Di Tullio, F.; Ciardo, S.; Chester, J.; Kaleci, S.; De Carvalho, N.; Del Duca, E.; Giannetti, L.; Mazzoni, L.; et al. Lesions Mimicking Melanoma at Dermoscopy Confirmed Basal Cell Carcinoma: Evaluation with Reflectance Confocal Microscopy. *Dermatology* **2018**, *235*, 35–44. [[CrossRef](#)]
50. Braga, J.C.T.; Scope, A.; Klaz, I.; Mecca, P.; González, S.; Rabinovitz, H.; Marghoob, A.A. The significance of reflectance confocal microscopy in the assessment of solitary pink skin lesions. *J. Am. Acad. Dermatol.* **2009**, *61*, 230–241. [[CrossRef](#)]
51. Longo, C.; Lallas, A.; Kyrgidis, A.; Rabinovitz, H.; Moscarella, E.; Ciardo, S.; Zalaudek, I.; Oliviero, M.; Losi, A.; Gonzalez, S.; et al. Classifying distinct basal cell carcinoma subtype by means of dermoscopy and reflectance confocal microscopy. *J. Am. Acad. Dermatol.* **2014**, *71*, 716–724. [[CrossRef](#)] [[PubMed](#)]
52. Rishpon, A.; Kim, N.; Scope, A.; Porges, L.; Oliviero, M.C.; Braun, R.P.; Marghoob, A.A.; Fox, C.A.; Rabinovitz, H.S. Reflectance Confocal Microscopy Criteria for Squamous Cell Carcinomas and Actinic Keratoses. *Arch. Dermatol.* **2009**, *145*, 766–772. [[CrossRef](#)]
53. Pellacani, G.; Ulrich, M.; Casari, A.; Prow, T.; Cannillo, F.; Benati, E.; Losi, A.; Cesinaro, A.; Longo, C.; Argenziano, G.; et al. Grading keratinocyte atypia in actinic keratosis: A correlation of reflectance confocal microscopy and histopathology. *J. Eur. Acad. Dermatol. Venereol.* **2015**, *29*, 2216–2221. [[CrossRef](#)]
54. Zalaudek, I.; Piana, S.; Moscarella, E.; Longo, C.; Zendri, E.; Castagnetti, F.; Pellacani, G.; Lallas, A.; Argenziano, G. Morphologic grading and treatment of facial actinic keratosis. *Clin. Dermatol.* **2014**, *32*, 80–87. [[CrossRef](#)]
55. Benati, E.; Pampena, R.; Bombonato, C.; Borsari, S.; Lombardi, M.; Longo, C. Dermoscopy and reflectance confocal microscopy for monitoring the treatment of actinic cheilitis with ingenol mebutate gel: Report of three cases. *Dermatol. Ther.* **2018**, *31*, e12613. [[CrossRef](#)] [[PubMed](#)]
56. Ulrich, M.; Kanitakis, J.; González, S.; Lange-Asschenfeldt, S.; Stockfleth, E.; Roewert-Huber, J. Evaluation of Bowen disease by in vivo reflectance confocal microscopy. *Br. J. Dermatol.* **2012**, *166*, 451–453. [[CrossRef](#)] [[PubMed](#)]
57. Shahriari, N.; Grant-Kels, J.M.; Rabinovitz, H.S.; Oliviero, M.; Scope, A. Reflectance confocal microscopy criteria of pigmented squamous cell carcinoma in situ. *Am. J. Dermatopathol.* **2018**, *40*, 173–179. [[CrossRef](#)] [[PubMed](#)]
58. Manfredini, M.; Longo, C.; Ferrari, B.; Piana, S.; Benati, E.; Casari, A.; Pellacani, G.; Moscarella, E. Dermoscopic and reflectance confocal microscopy features of cutaneous squamous cell carcinoma. *J. Eur. Acad. Dermatol. Venereol.* **2017**, *31*, 1828–1833. [[CrossRef](#)] [[PubMed](#)]
59. Champin, J.; Perrot, J.-L.; Cinotti, E.; Labeille, B.; Douchet, C.; Parrau, G.; Cambazard, F.; Seguin, P.; Alix, T. In vivo reflectance confocal microscopy to optimize the spaghetti technique for defining surgical margins of lentigo maligna. *Dermatol. Surg.* **2014**, *40*, 247–256. [[CrossRef](#)]
60. Guitera, P.; Moloney, F.J.; Menzies, S.W.; Stretch, J.R.; Quinn, M.J.; Hong, A.; Fogarty, G.; Scolyer, R.A. Improving Management and Patient Care in Lentigo Maligna by Mapping With In Vivo Confocal Microscopy. *JAMA Dermatol.* **2013**, *149*, 692–698. [[CrossRef](#)] [[PubMed](#)]
61. Farnetani, F.; Manfredini, M.; Chester, J.; Ciardo, S.; Gonzalez, S.; Pellacani, G. Reflectance confocal microscopy in the diagnosis of pigmented macules of the face: Differential diagnosis and margin definition. *Photochem. Photobiol. Sci.* **2019**, *18*, 963–969. [[CrossRef](#)]
62. Yélamos, O.; Cordova, M.; Blank, N.; Kose, K.; Dusza, S.W.; Lee, E.; Rajadhyaksha, M.; Nehal, K.S.; Rossi, A.M. Correlation of Handheld Reflectance Confocal Microscopy With Radial Video Mosaicing for Margin Mapping of Lentigo Maligna and Lentigo Maligna Melanoma. *JAMA Dermatol.* **2017**, *153*, 1278–1284. [[CrossRef](#)]
63. Navarrete-Dechent, C.; Cordova, M.; AlEissa, S.; Liopyris, K.; Dusza, S.W.; Kose, K.; Busam, K.J.; Hollman, T.; Lezcano, C.; Pulitzer, M.; et al. Lentigo maligna melanoma mapping using reflectance confocal microscopy correlates with staged excision: A prospective study. *J. Am. Acad. Dermatol.* **2019**, S0190-9622(19)33150-0. [[CrossRef](#)]
64. Venturini, M.; Gualdi, G.; Zanca, A.; Lorenzi, L.; Pellacani, G.; Calzavara-Pinton, P.G. A new approach for presurgical margin assessment by reflectance confocal microscopy of basal cell carcinoma. *Br. J. Dermatol.* **2015**, *174*, 380–385. [[CrossRef](#)]
65. Lupu, M.; Voiculescu, V.; Caruntu, A.; Tebeica, T.; Caruntu, C. Preoperative Evaluation through Dermoscopy and Reflectance Confocal Microscopy of the Lateral Excision Margins for Primary Basal Cell Carcinoma. *Diagnostics* **2021**, *11*, 120. [[CrossRef](#)]
66. Grajdeanu, I.; Statescu, L.; Vata, D.; Popescu, I.A.; Porumb-Andrese, E.; Patrascu, A.I.; Taranu, T.; Crisan, M.; Solovastru, L.G. Imaging techniques in the diagnosis and monitoring of psoriasis (Review). *Exp. Ther. Med.* **2019**, *18*, 4974–4980. [[CrossRef](#)] [[PubMed](#)]
67. Ardigo, M.; Malizewsky, I.; Dell’Anna, M.; Berardesca, E.; Picardo, M. Preliminary evaluation of vitiligo using in vivo reflectance confocal microscopy. *J. Eur. Acad. Dermatol. Venereol.* **2007**, *21*, 1344–1350. [[CrossRef](#)] [[PubMed](#)]
68. Ardigo, M.; Cameli, N.; Berardesca, E.; González, S. Characterization and evaluation of pigment distribution and response to therapy in melasma using in vivo reflectance confocal microscopy: A preliminary study. *J. Eur. Acad. Dermatol. Venereol.* **2010**, *24*, 1296–1303. [[CrossRef](#)]
69. Longo, C.; Casari, A.; Beretti, F.; Cesinaro, A.M.; Pellacani, G. Skin aging: In vivo microscopic assessment of epidermal and dermal changes by means of confocal microscopy. *J. Am. Acad. Dermatol.* **2013**, *68*, e73–e82. [[CrossRef](#)] [[PubMed](#)]
70. Rovatti, P.P.; Pellacani, G.; Guida, S. Hyperdiluted Calcium Hydroxylapatite 1: 2 for Mid and Lower Facial Skin Reju-venation: Efficacy and Safety. *Dermatol. Surg.* **2020**, *46*, e112–e117. [[CrossRef](#)] [[PubMed](#)]
71. Marco, M.; Giovanna, M.; Silvana, C.; Silvia, S.; Francesca, F.; Caterina, L.; Giovanni, P. Does skin hydration influence keratinocyte biology? In vivo evaluation of microscopic skin changes induced by moisturizers by means of Reflectance Confocal Microscopy. *Ski. Res. Technol.* **2013**, *19*, 299–307. [[CrossRef](#)]

72. Manfredini, M.; Mazzaglia, G.; Ciardo, S.; Farnetani, F.; Mandel, V.D.; Longo, C.; Zauli, S.; Bettoli, V.; Virgili, A.; Pellacani, G. Acne: In vivo morphologic study of lesions and surrounding skin by means of reflectance confocal microscopy. *J. Eur. Acad. Dermatol. Venereol.* **2015**, *29*, 933–939. [[CrossRef](#)] [[PubMed](#)]
73. Manfredini, M.; Greco, M.; Farnetani, F.; Mazzaglia, G.; Ciardo, S.; Bettoli, V.; Virgili, A.; Pellacani, G. In vivo monitoring of topical therapy for acne with reflectance confocal microscopy. *Ski. Res. Technol.* **2016**, *23*, 36–40. [[CrossRef](#)] [[PubMed](#)]
74. Guida, S.; Pellacani, G.; Bencini, P.L. Picosecond laser treatment of atrophic and hypertrophic surgical scars: In vivo monitoring of results by means of 3D imaging and reflectance confocal microscopy. *Ski. Res. Technol.* **2019**, *25*, 896–902. [[CrossRef](#)]
75. Ardigò, M.; Longo, C.; González, S. Multicenter study on inflammatory skin diseases from The International Confocal Working Group (ICG): Specific confocal microscopy features and an algorithmic method of diagnosis. *Br. J. Dermatol.* **2016**, *175*, 364–374. [[CrossRef](#)] [[PubMed](#)]
76. Longo, C.; Pellacani, G.; Tourlaki, A.; Galimberti, M.; Bencini, P.L. Melasma and low-energy Q-switched laser: Treatment assessment by means of in vivo confocal microscopy. *Lasers Med. Sci.* **2014**, *29*, 1159–1163. [[CrossRef](#)] [[PubMed](#)]
77. Longo, C.; Galimberti, M.; De Pace, B.; Pellacani, G.; Bencini, P.L. Laser skin rejuvenation: Epidermal changes and collagen remodeling evaluated by in vivo confocal microscopy. *Lasers Med. Sci.* **2012**, *28*, 769–776. [[CrossRef](#)]
78. Guida, S.; Bencini, P.; Pellacani, G. Picosecond laser for atrophic surgical scars treatment: In vivo monitoring of results by means of reflectance confocal microscopy. *J. Eur. Acad. Dermatol. Venereol.* **2018**, *33*, e114–e116. [[CrossRef](#)]
79. Guida, S.; Losi, A.; Greco, M.; Ciardo, S.; Pellacani, G.; Longo, C. Reflectance confocal microscopy for striae distansae treatment monitoring after CO₂ fractional laser. *Dermatol. Ther.* **2020**, *33*, 14318. [[CrossRef](#)] [[PubMed](#)]
80. Guida, S.; Galimberti, M.G.; Bencini, M.; Pellacani, G.; Bencini, P.L. Treatment of striae distansae with non-ablative fractional laser: Clinical and in vivo microscopic documentation of treatment efficacy. *Lasers Med. Sci.* **2017**, *33*, 75–78. [[CrossRef](#)] [[PubMed](#)]
81. Manfredini, M.; Bettoli, V.; Sacripanti, G.; Farnetani, F.; Bigi, L.; Puviani, M.; Corazza, M.; Pellacani, G. The evolution of healthy skin to acne lesions: A longitudinal, in vivo evaluation with reflectance confocal microscopy and optical coherence tomography. *J. Eur. Acad. Dermatol. Venereol.* **2019**, *33*, 1768–1774. [[CrossRef](#)] [[PubMed](#)]
82. Cinotti, E.; Perrot, J.L.; Labeille, B.; Cambazard, F.; Rubegni, P. Ex vivo confocal microscopy: An emerging technique in dermatology. *Dermatol. Pract. Concept.* **2018**, *8*, 109–119. [[CrossRef](#)]
83. Longo, C.; Borsari, S.; Pampena, R.; Benati, E.; Bombonato, C.; Raucci, M.; Mirra, M.; Di Stefani, A.; Peris, K.; Pellacani, G. Basal cell carcinoma: The utility of in vivo and ex vivo confocal microscopy. *J. Eur. Acad. Dermatol. Venereol.* **2018**, *32*, 2090–2096. [[CrossRef](#)] [[PubMed](#)]
84. Longo, C.; Ragazzi, M.; Rajadhyaksha, M.; Nehal, K.; Bennassar, A.; Pellacani, G.; Guilera, J.M. In Vivo and Ex Vivo Confocal Microscopy for Dermatologic and Mohs Surgeons. *Dermatol. Clin.* **2016**, *34*, 497–504. [[CrossRef](#)] [[PubMed](#)]
85. Iovieno, A.; Longo, C.; De Luca, M.; Piana, S.; Fontana, L.; Ragazzi, M. Fluorescence Confocal Microscopy for Ex Vivo Diagnosis of Conjunctival Tumors: A Pilot Study. *Am. J. Ophthalmol.* **2016**, *168*, 207–216. [[CrossRef](#)] [[PubMed](#)]
86. Bini, J.; Spain, J.; Nehal, K.; Hazelwood, V.; DiMarzio, C.; Rajadhyaksha, M. Confocal mosaicing microscopy of human skin ex vivo: Spectral analysis for digital staining to simulate histology-like appearance. *J. Biomed. Opt.* **2011**, *16*, 076008. [[CrossRef](#)]
87. Cinotti, E.; Belgrano, V.; Labeille, B.; Grivet, D.; Douchet, C.; Chauleur, C.; Cambazard, F.; Thomas, A.; Prade, V.; Tognetti, L.; et al. In vivo and ex vivo confocal microscopy for the evaluation of surgical margins of melanoma. *J. Biophotonics* **2020**, *13*, e202000179. [[CrossRef](#)]
88. Ragazzi, M.; Piana, S.; Longo, C.; Castagnetti, F.; Foroni, M.; Ferrari, G.; Gardini, G.; Pellacani, G. Fluorescence confocal microscopy for pathologists. *Mod. Pathol.* **2013**, *27*, 460–471. [[CrossRef](#)]
89. Gareau, D.S. Feasibility of digitally stained multimodal confocal mosaics to simulate histopathology. *J. Biomed. Opt.* **2009**, *14*, 034050. [[CrossRef](#)]
90. Pérez-Anker, J.; Malvehy, J.; Moreno-Ramírez, D. Ex Vivo Confocal Microscopy Using Fusion Mode and Digital Staining: Changing Paradigms in Histological Diagnosis. *Actas Dermo-Sifiliográficas* **2020**, *111*, 236–242. [[CrossRef](#)] [[PubMed](#)]
91. Mercuri, S.R.; Rizzo, N.; Bellinzona, F.; Pampena, R.; Brianti, P.; Moffa, G.; Flink, L.C.; Bearzi, P.; Longo, C.; Paolino, G.; et al. Digital ex-vivo confocal imaging for fast Mohs surgery in nonmelanoma skin cancers: An emerging technique in dermatologic surgery. *Dermatol. Ther.* **2019**, *32*, e13127. [[CrossRef](#)] [[PubMed](#)]
92. Longo, C.; Rajadhyaksha, M.; Ragazzi, M.; Nehal, K.; Gardini, S.; Moscarella, E.; Lallas, A.; Zalaudek, I.; Piana, S.; Argenziano, G.; et al. Evaluating ex vivo fluorescence confocal microscopy images of basal cell carcinomas in Mohs excised tissue. *Br. J. Dermatol.* **2014**, *171*, 561–570. [[CrossRef](#)]
93. Longo, C.; Ragazzi, M.; Castagnetti, F.; Gardini, S.; Palmieri, T.; Lallas, A.; Moscarella, E.; Piana, S.; Pellacani, G.; Zalaudek, I.; et al. Inserting ex vivo Fluorescence Confocal Microscopy Perioperatively in Mohs Micrographic Surgery Expedites Bedside Assessment of Excision Margins in Recurrent Basal Cell Carcinoma. *Dermatology* **2013**, *227*, 89–92. [[CrossRef](#)] [[PubMed](#)]
94. Hartmann, D.; Ruini, C.; Mathemeier, L.; Dietrich, A.; Ruzicka, T.; Von Braunmühl, T. Identification of ex-vivo confocal scanning microscopic features and their histological correlates in human skin. *J. Biophotonics* **2016**, *9*, 376–387. [[CrossRef](#)] [[PubMed](#)]
95. Cinotti, E.; Labeille, B.; Cambazard, F.; Perrot, J.-L. Confocal Microscopy for Special Sites and Special Uses. *Dermatol. Clin.* **2016**, *34*, 477–485. [[CrossRef](#)] [[PubMed](#)]
96. Cinotti, E.; Fouilloux, B.; Perrot, J.L.; Labeille, B.; Douchet, C.; Cambazard, F. Confocal microscopy for healthy and pathological nail. *J. Eur. Acad. Dermatol. Venereol.* **2014**, *28*, 853–858. [[CrossRef](#)]

97. Cinotti, E.; Perrot, J.L.; Labeille, B.; Campolmi, N.; Thuret, G.; Naigeon, N.; Bourlet, T.; Pillet, S.; Cambazard, F. First identification of the herpes simplex virus by skin-dedicated ex vivo fluorescence confocal microscopy during herpetic skin infections. *Clin. Exp. Dermatol.* **2015**, *40*, 421–425. [[CrossRef](#)]
98. El Hallani, S.; Poh, C.F.; Macaulay, C.E.; Follen, M.; Guillaud, M.; Lane, P. Ex vivo confocal imaging with contrast agents for the detection of oral potentially malignant lesions. *Oral Oncol.* **2013**, *49*, 582–590. [[CrossRef](#)]
99. Bertoni, L.; Azzoni, P.; Reggiani, C.; Pisciotta, A.; Carnevale, G.; Chester, J.; Kaleci, S.; Bonetti, L.R.; Cesinaro, A.M.; Longo, C.; et al. Ex vivo fluorescence confocal microscopy for intraoperative, real-time diagnosis of cutaneous inflammatory diseases: A preliminary study. *Exp. Dermatol.* **2018**, *27*, 1152–1159. [[CrossRef](#)] [[PubMed](#)]
100. Cinotti, E.; Perrot, J.L.; Labeille, B.; Boukenter, A.; Ouerdane, Y.; Cosmo, P.; Douchet, C.; Grivet, D.; Cambazard, F. Identification of a soft tissue filler by ex vivo confocal microscopy and Raman spectroscopy in a case of adverse reaction to the filler. *Ski. Res. Technol.* **2014**, *21*, 114–118. [[CrossRef](#)] [[PubMed](#)]
101. Malvehy, J.; Pérez-Anker, J.; Toll, A.; Pigem, R.; Garcia, A.; Alos, L.; Puig, S. Ex vivo confocal microscopy: Revolution in fast pathology in dermatology. *Br. J. Dermatol.* **2020**, *183*, 1011–1025. [[CrossRef](#)]
102. Ortner, V.K.; Sahu, A.; Haedersdal, M.; Rajadhyaksha, M.; Rossi, A.M. Assessment of laser-induced thermal damage in fresh skin with ex vivo confocal microscopy. *J. Am. Acad. Dermatol.* **2021**, *84*, e19–e21. [[CrossRef](#)]
103. Hartmann, D.; Krammer, S.; Vural, S.; Bachmann, M.R.; Ruini, C.; Sárdy, M.; Ruzicka, T.; Berking, C.; Von Braunmühl, T. Immunofluorescence and confocal microscopy for ex-vivo diagnosis of melanocytic and non-melanocytic skin tumors: A pilot study. *J. Biophotonics* **2017**, *11*, e201700211. [[CrossRef](#)] [[PubMed](#)]
104. Bağcı, I.S.; Aoki, R.; Krammer, S.; Ruzicka, T.; Sárdy, M.; Hartmann, D. Ex vivo confocal laser scanning microscopy: An innovative method for direct immunofluorescence of cutaneous vasculitis. *J. Biophotonics* **2019**, *12*, e201800425. [[CrossRef](#)]
105. Bağcı, I.S.; Aoki, R.; Krammer, S.; Ruzicka, T.; Sárdy, M.; French, L.E.; Hartmann, D. Ex vivo confocal laser scanning microscopy for bullous pemphigoid diagnostics: New era in direct immunofluorescence? *J. Eur. Acad. Dermatol. Venereol.* **2019**, *33*, 2123–2130. [[CrossRef](#)] [[PubMed](#)]
106. Bennàssar, A.; Carrera, C.; Puig, S.; Vilalta, A.; Malvehy, J. Fast Evaluation of 69 Basal Cell Carcinomas With Ex Vivo Fluorescence Confocal Microscopy: Criteria description, histopathological correlation, and interobserver agreement. *JAMA Dermatol.* **2013**, *149*, 839–847. [[CrossRef](#)] [[PubMed](#)]
107. Longo, C.; Pampena, R.; Bombonato, C.; Gardini, S.; Piana, S.; Mirra, M.; Raucci, M.; Kyrgidis, A.; Pellacani, G.; Ragazzi, M. Diagnostic accuracy of ex vivo fluorescence confocal microscopy in Mohs surgery of basal cell carcinomas: A prospective study on 753 margins. *Br. J. Dermatol.* **2019**, *180*, 1473–1480. [[CrossRef](#)] [[PubMed](#)]
108. Villarreal-Martinez, A.; Bennàssar, A.; Gonzalez, S.; Malvehy, J.; Puig, S. Application of in vivo reflectance confocal microscopy and ex vivo fluorescence confocal microscopy in the most common subtypes of basal cell carcinoma and correlation with histopathology. *Br. J. Dermatol.* **2018**, *178*, 1215–1217. [[CrossRef](#)]
109. Longo, C.; Ragazzi, M.; Gardini, S.; Piana, S.; Moscarella, E.; Lallas, A.; Raucci, M.; Argenziano, G.; Pellacani, G. Ex vivo fluorescence confocal microscopy in conjunction with Mohs micrographic surgery for cutaneous squamous cell carcinoma. *J. Am. Acad. Dermatol.* **2015**, *73*, 321–322. [[CrossRef](#)]
110. Hartmann, D.; Krammer, S.; Bachmann, M.R.; Mathemeier, L.; Ruzicka, T.; Bağcı, I.S.; Von Braunmühl, T. Ex vivo confocal microscopy features of cutaneous squamous cell carcinoma. *J. Biophotonics* **2018**, *11*, e201700318. [[CrossRef](#)] [[PubMed](#)]
111. Mentzel, J.; Stecher, M.; Paasch, U.; Simon, J.C.; Grunewald, S. Ex-vivo confocal laser scanning microscopy with digital staining is able to map characteristic histopathological features and tissue reaction patterns of inflammatory skin diseases. *J. Eur. Acad. Dermatol. Venereol.* **2020**. [[CrossRef](#)] [[PubMed](#)]
112. Krishnamurthy, S.; Cortes, A.; Lopez, M.; Wallace, M.; Sabir, S.; Shaw, K.; Mills, G. Ex Vivo Confocal Fluorescence Microscopy for Rapid Evaluation of Tissues in Surgical Pathology Practice. *Arch. Pathol. Lab. Med.* **2017**, *142*, 396–401. [[CrossRef](#)] [[PubMed](#)]
113. Puliatti, S.; Bertoni, L.; Pirola, G.M.; Azzoni, P.; Bevilacqua, L.; Eissa, A.; Elsherbiny, A.; Sighinolfi, M.C.; Chester, J.; Kaleci, S.; et al. Ex vivo fluorescence confocal microscopy: The first application for real-time pathological examination of prostatic tissue. *BJU Int.* **2019**, *124*, 469–476. [[CrossRef](#)] [[PubMed](#)]
114. Bertoni, L.; Puliatti, S.; Bonetti, L.R.; Maiorana, A.; Eissa, A.; Azzoni, P.; Bevilacqua, L.; Spandri, V.; Kaleci, S.; Zoeir, A.; et al. Ex vivo fluorescence confocal microscopy: Prostatic and periprostatic tissues atlas and evaluation of the learning curve. *Virchows Arch.* **2020**, *476*, 511–520. [[CrossRef](#)]